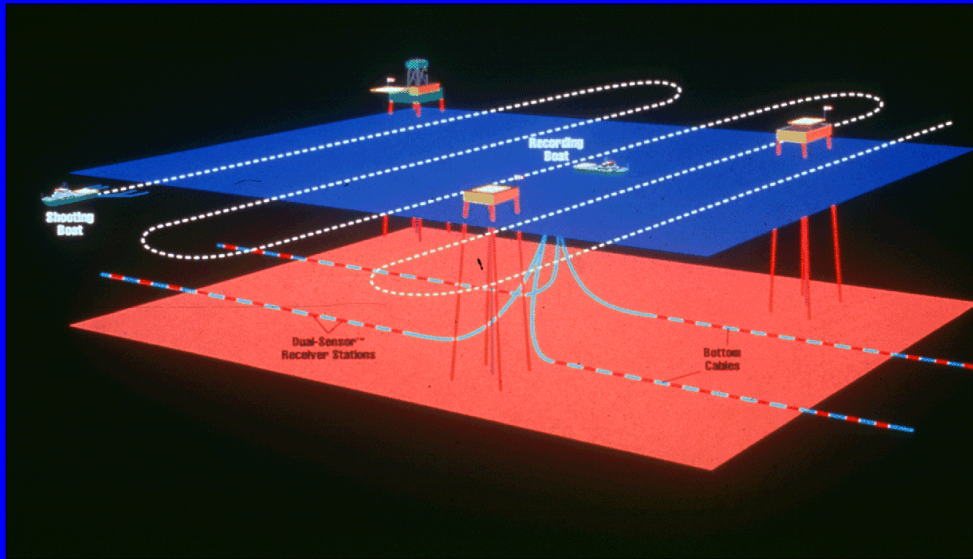


Modeling Velocity Gradients in an OBC, First-Break Positioning Algorithm

Noel Zinn
Western Geophysical
EAGE Geneva 1997

In this talk I provide an overview of the modeling of vertical and lateral velocity gradients that can be sources of systematic error in Ocean Bottom Cable first-break positioning algorithms. The mathematics of the solutions I propose are detailed in the paper accompanying this overview. My thesis is simple. By modeling sources of systematic error and by compensating for random first-break quality with a large number of observations, first-break coordinates can be as accurate as acoustics at less cost.

Orthogonal Shooting Style



By way of orientation I first show a schematic of the orthogonal shooting style in OBC. There are cables with dual sensor detectors on the bottom connected to a recording and processing vessel shown in the middle. The shooting vessel sailing perpendicularly to the swath is on the left. This orthogonal style has certain geophysical and geodetic advantages, but in-line shooting is also possible.

Shooting Vessel with Towed Source



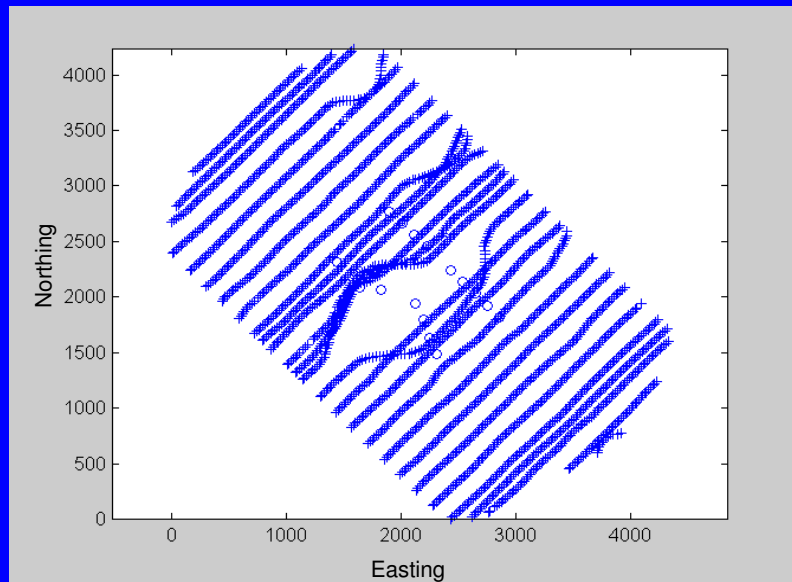
This picture shows the stern of a shooting vessel towing a source array. Notice the GPS antenna positioning the source array.

Stern of Cable-Laying Vessel



This picture is the back deck of a cable laying vessel showing the "squirter" at center stern for deploying the cables.

Real-Data Swath Subset



This graphic shows a subset of a real-data swath that is extensively analyzed in this paper. There are just 16 detectors that are coupled with acoustic sensors shown as circles and 2500 orthogonally-fired shots shown as plus signs. Notice that this swath was shot around obstructions, an excellent use of OBC.

Methods of Positioning OBC Detectors

- 1 Drop positions (inexpensive but imprecise)
- 2 Acoustics (expensive but precise)
- 3 First breaks (inexpensive and precise)
 - Combination of first breaks and acoustics

Source positioning in OBC is similar in technique and quality to source positioning in deep-water streamer surveys. It basically consists of GPS antennas on the source array. On the other hand, detector positioning techniques are less-widely standardized. Three techniques are common in the industry. (1) Recording and using the drop coordinates of the detectors. This is inexpensive, but often imprecise. (2) Deploying high-frequency acoustic sensors attached to all or some of the detectors and positioned by a “pinging” survey independent of the seismic survey. This technique is expensive and time consuming, but, properly executed, can be precise. Or (3) using multiple occasions of the onset of seismic energy (called first breaks) as surveying observations in a positioning algorithm. This technique is inexpensive because the data, personnel and software are already on the vessel to reposition the swath immediately after shooting. Because we have so many first-break picks, it can be very precise as the laws of statistical error cancellation confirm. A combination of first breaks and acoustics is also possible.

Acoustic Error Sources

- Detector depth
- Velocity of propagation
- Inadequate number of pings
- Inadequate geometry
- Instrumental delay
- Surface “ghosts”
- Vessel noise
- Muddy bottoms

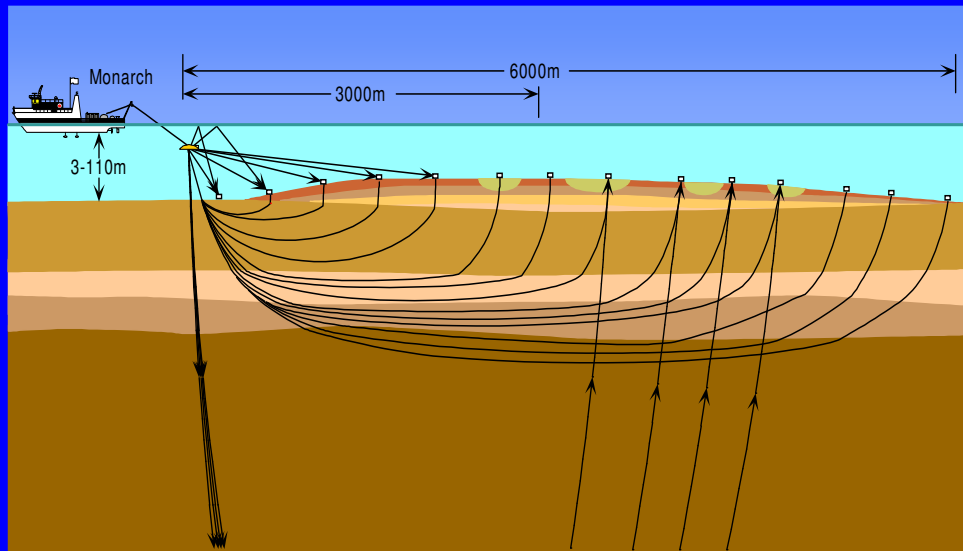
In analyses that follow, I compare acoustic and first-break results. So it is appropriate to overview some of the significant error sources associated with each of these systems. Although acoustics provide a precise observable with low random error, positions can be systematically affected by incorrect detector depths for computing the slant range correction, by an incorrect knowledge of the velocity of acoustic propagation in water (especially due to thermal layering), by pinging too few times or in bad geometry or both, by instrumental delay, by multi-path (specifically surface "ghosts"), by interfering vessel noise and by muddy bottoms that mask the signal.

First-Break Error Sources

- Random error (2 - 6 ms per pick)
- Source array dimensions and orientation
- Instrumental delay
- Definition of energy onset
- Vertical velocity gradient (water & refractors)
- Lateral velocity gradient
- Anomalous near-surface geology

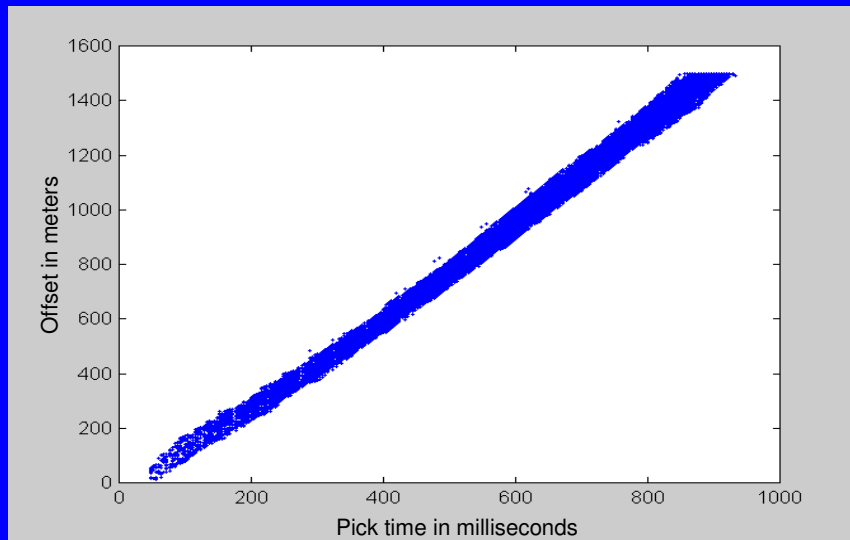
On the other hand, first-break errors sources are a crude observable that may be good only to 3 to 9 meters or worse in a random sense, but we have a lot of them. Given source-array dimensions and pick azimuth, simple programming can determine which gun at what coordinates generated the onset of energy. Instrumental delay is also an issue. Different first-break pickers may have different mathematical definitions of the onset of seismic energy. I will explain in a moment what I mean by vertical and lateral velocity gradients. A complex near-surface geology can be the toughest of all, when it occurs. In this talk and in the accompanying paper I offer compensations for all these sources of first-break positioning error.

Vertical Velocity Gradient



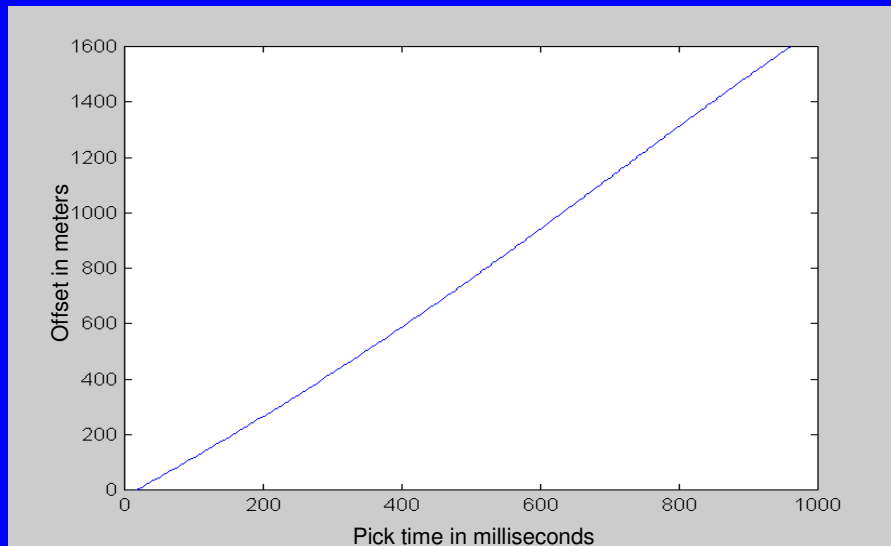
This graphic explains a vertical gradient. It shows a single source event and the many paths the seismic energy may take to arrive first at each detector. Some detectors will see the energy first directly through the water. But because the sedimentary layers may have velocities that increase with depth, the first break may arrive through one or more of these refractive layers. Our objective is to use all this information in one automated positioning algorithm.

Offset versus Pick Time



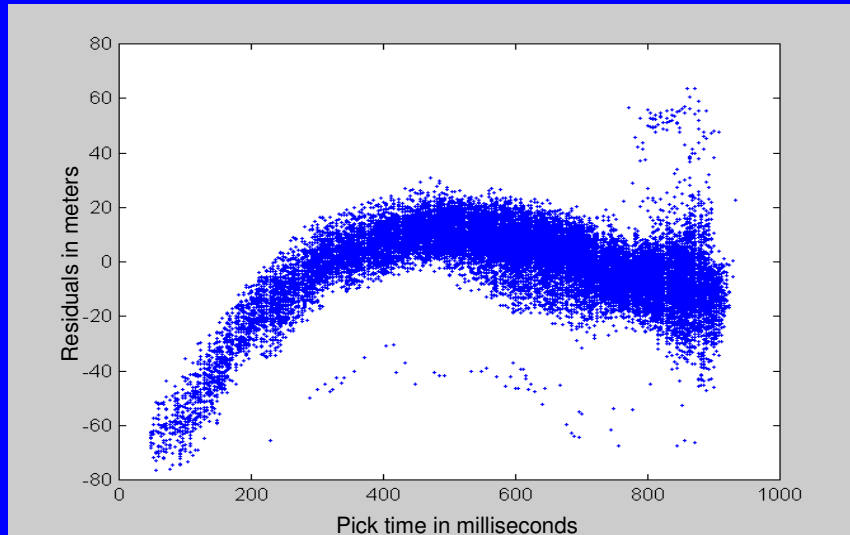
For the swath subset already seen, this graphic shows all pick offsets in meters on the Y axis plotted against all pick travel times in milliseconds before repositioning. Offsets are defined as the Pythagorean distance between the source and drop coordinates. The pick times are our observations. There are 23,000 of them.

Vertical-Gradient Polynomial



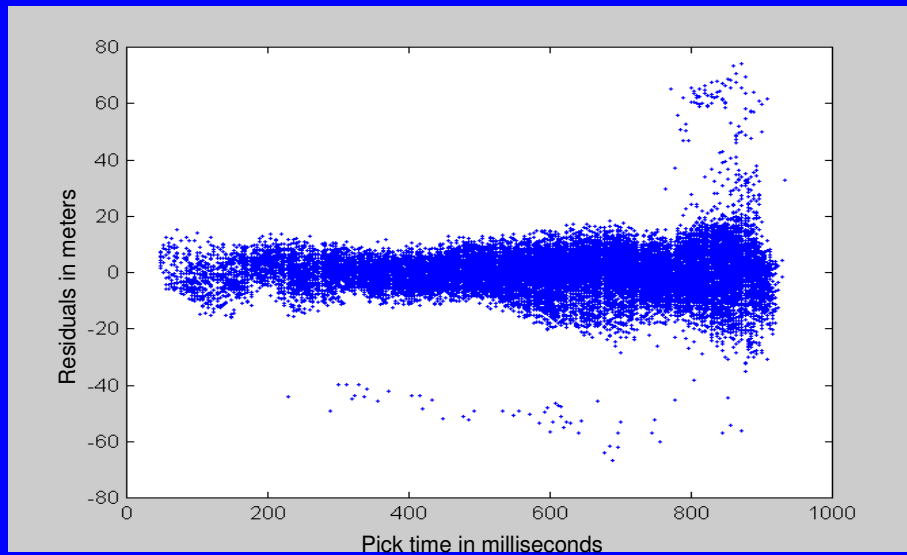
Modeling the vertical gradient is accomplished by fitting these data with a polynomial of order sufficient to flatten the residuals. Such a polynomial is shown in this graphic. Notice that the polynomial does not cross the origin. The Y intercept at zero pick time absorbs two of the error sources previously mentioned, namely, instrumental delay and the definition of the onset of energy in the first-break picker.

Real-Data, First-Order Residual Plot



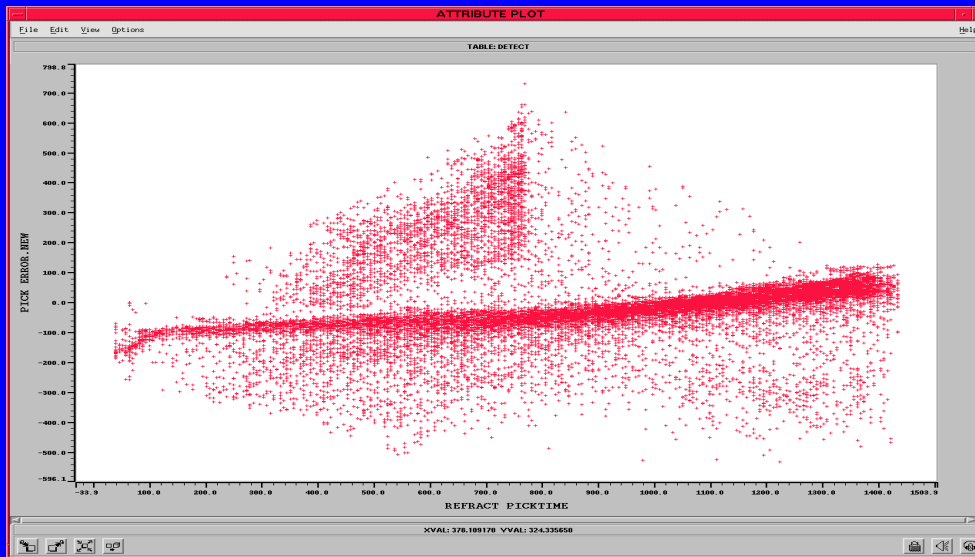
A residual is an important concept in geodetic adjustment theory. A residual is the C-O, the computed minus the observed. In this case it is the computed Pythagorean distance (or offset) for a given source-detector pair minus the distance corresponding to the related pick time substituted into the best fitting polynomial, in other words, the picks less the profile. This graphic is a residual plot. Residuals in meters on the Y axis are plotted against pick times in milliseconds on the X axis. A first-order, linear polynomial was used to generate this plot. In other words, the vertical gradient is not modeled. The trend as a function of pick time is obvious. Variation in the velocity of propagation as a function of pick time and depth of refractor, can be implied from this plot. Our objective is to flatten the residual plot.

Real-Data, Fifth-Order Residual Plot



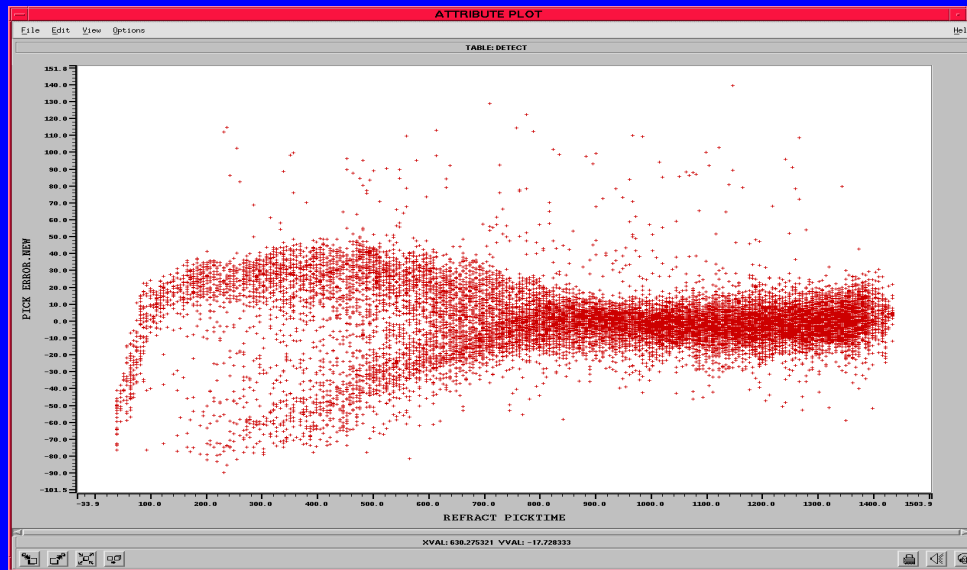
This is accomplished with a fifth-order polynomial to produce this graphic. Residuals are now zero mean over all offsets. Some outliers are shown. They can now be easily distinguished from the good data and rejected. The first differential of the best-fitting polynomial provides an equation of average velocity as a function of pick time. In other words, the vertical gradient is modeled.

Omega Residuals without Pick Rejection



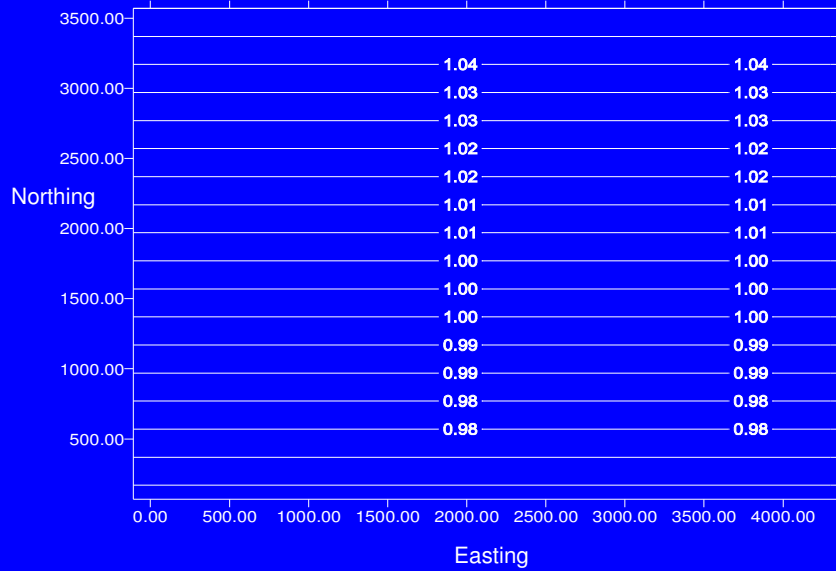
This residual plots from Western's Omega processing system (and the next slide, too) show another prospect with poorer-quality picks. No outlier rejection is applied in this slide. Outlier rejection is applied in the next slide. Although it is hard to read, residuals on the Y axis span approximately plus/minus 700 meters (this slide) and plus/minus 100 meters (next slide). It is obvious that pick rejection and a third-order vertical polynomial clean up the data on the next slide, now centered about zero for all offsets. Notice that some complex, near-surface geology is exhibited in the near offsets on the next slide, with the far offsets behaving much better through the deeper travel paths.

Omega Residuals with Pick Rejection



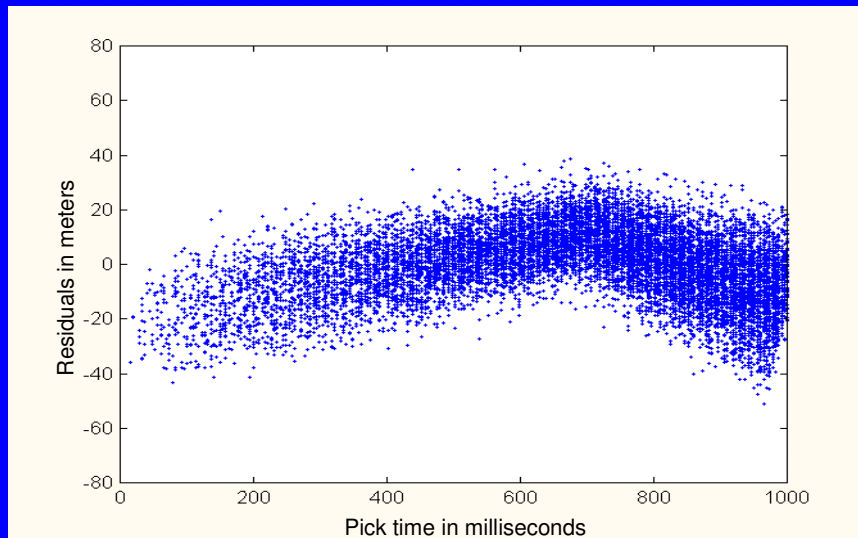
A lateral (or horizontal) velocity gradient is a variation in velocity as a function of position in a prospect. Different than anisotropy, it may be uniform in all directions at a specific point, but vary over the entire prospect. A lateral gradient behaves like scale factor in what cartographers refer to as a conformal map projection. It may be caused, for example, by a greater compaction of the recent sedimentation as one moves farther offshore. Since the refracted energy used in OBC first-break positioning primarily travels through the recent sedimentary layers, a lateral gradient may sometimes be a factor in positioning results. A simple least-squares algorithm will give erroneous results in the presence of a lateral gradient, with coordinates biased in the direction of the gradient.

Simulated Lateral Velocity Gradient



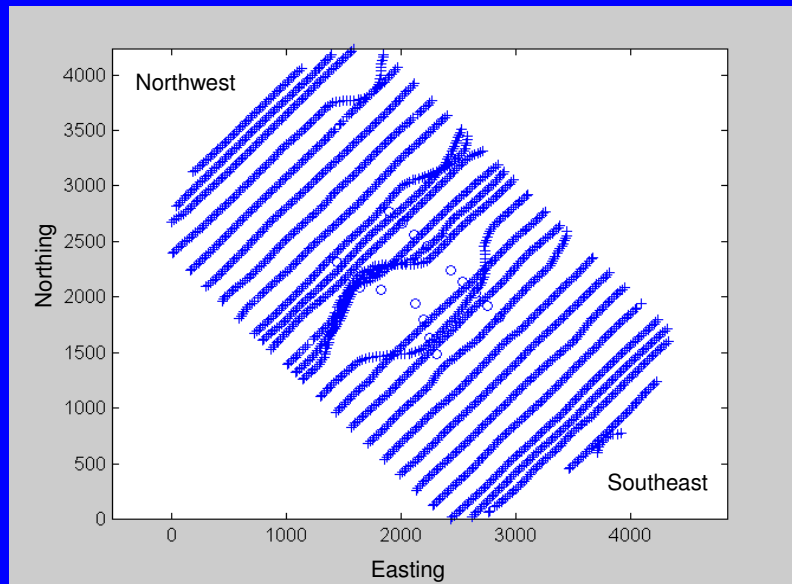
This graphic shows a simulated lateral gradient. It's linear, relatively mild and all in the Y coordinate. Since the global vertical velocity trend has already been removed by the vertical profile, this gradient appears as numbers near unity, like the scale factors on a map.

Simulated-Data Residual Plot



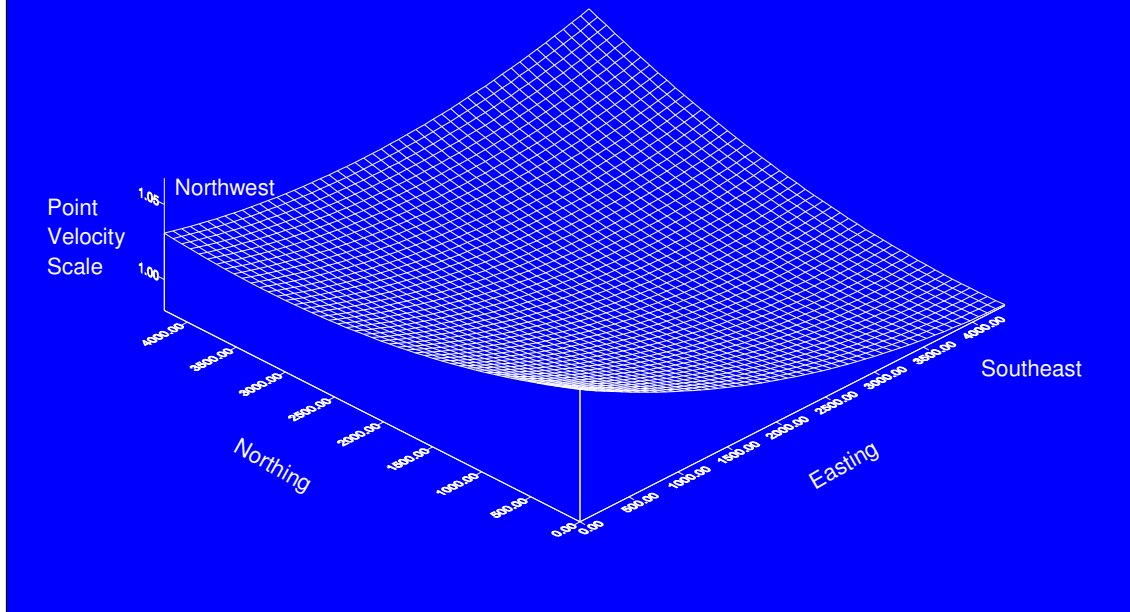
This graphic is a residual plot of synthetic data created using the lateral gradient on the previous slide. The simulator models direct water arrivals and three distinct refractors that produce a vertical gradient. A normally distributed random error of 4 milliseconds (one sigma) is added to the simulated picks. The picks are then rounded to the nearest 4 milliseconds to emulate a commonly-used sampling interval that produces excellent positioning results. The effect of the vertical gradient is obvious in this graphic, which was computed with a linear vertical profile. Since the velocity in each refractor is constant throughout its thickness in the simulator, one refractor “break” is quite distinct. This sometimes occurs similarly in nature. These data will be visited again in the comparisons that follow.

Real-Data Swath Subset



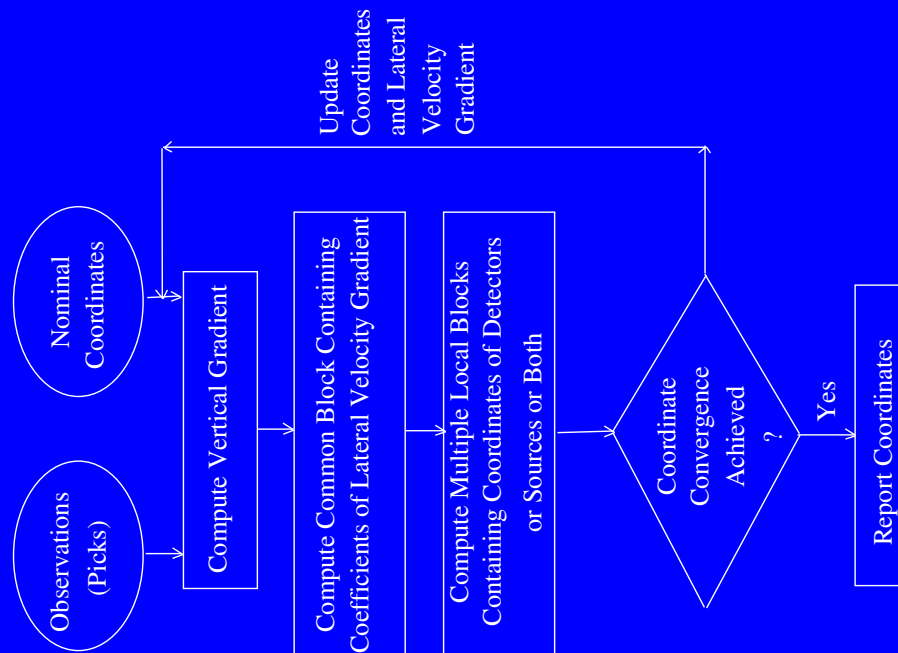
Now we return to this real-data example.

Real-Data Computed Lateral-Velocity Gradient



This graphic shows the lateral gradient computed from the real data prospect of the previous slide. It is shown as a quadratic surface, a two-dimensional polynomial in X and Y coordinates. The mathematics for computing this surface are derived in the accompanying paper. Notice the gradient from north-west to south-east, the direction of this swath subset. The peaks in the north-east and south-west are artifacts of extrapolating the quadratic surface into territory unconstrained by real data.

Helmert Flow Diagram



This graphic is a flow diagram of the algorithm I call Helmert because it uses the geodetic adjustment technique of Helmert-blocking for computational efficiency. We start with our picks and our nominal coordinates. The global vertical gradient for all picks in the entire swath is computed as previously described. Then, in a simultaneous, network adjustment of all data, the coefficients of the lateral gradient are computed. Using some intermediate matrix products, the coordinates of all detectors are computed. If convergence to some pre-defined tolerance is achieved, we are done. If not, the nominal coordinates and the coefficients of the lateral gradient are updated and iteration continues until convergence.

Verification of Positioning Algorithm

- 1 Comparison with truth (synthetic data)
- 2 Comparison with acoustics (real data)
- 3 Data splitting into independent data samples (real or synthetic data)
 - Randomly over entire offset range
 - Near offsets versus far offsets

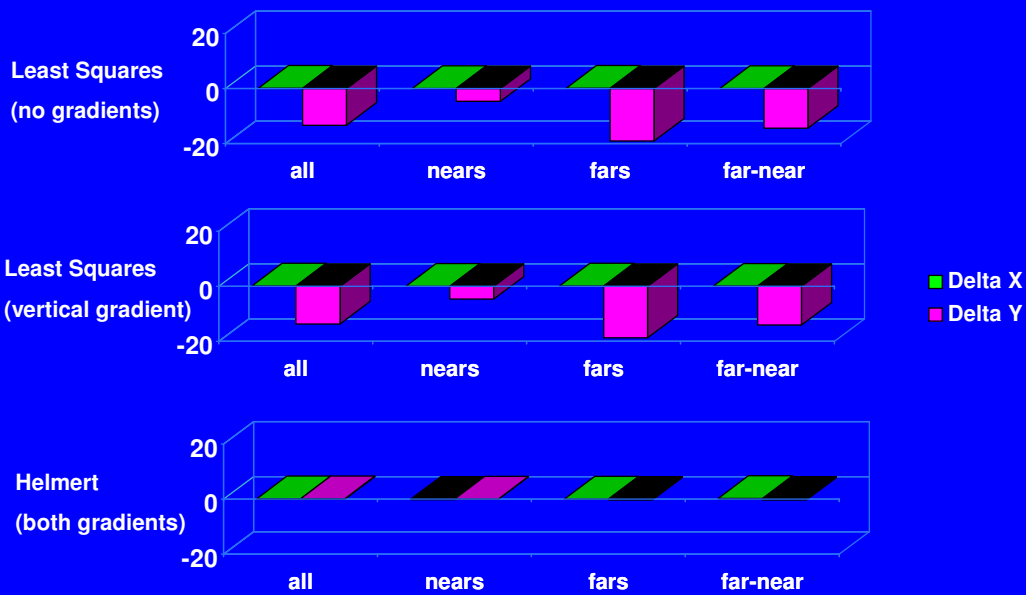
We can verify the efficacy of this approach in three ways: by comparison with truth using synthetic data, by comparison with acoustics using real data, and by splitting the picks into independent samples and comparing results. Such splits can be made randomly over the entire offset range or by dividing on offset into nears and fars. Random splits always agree extremely well. Offset splits are a greater challenge that have important implications for dealing with an anomalous near-surface geology.

Algorithms Tested

- 1 Simple least squares (LS) with linear vertical profile
- 2 Simple least squares (LS) with higher-order vertical profile
- 3 Complex least squares (Helmert) with both higher-order vertical profile and quadratic lateral gradient

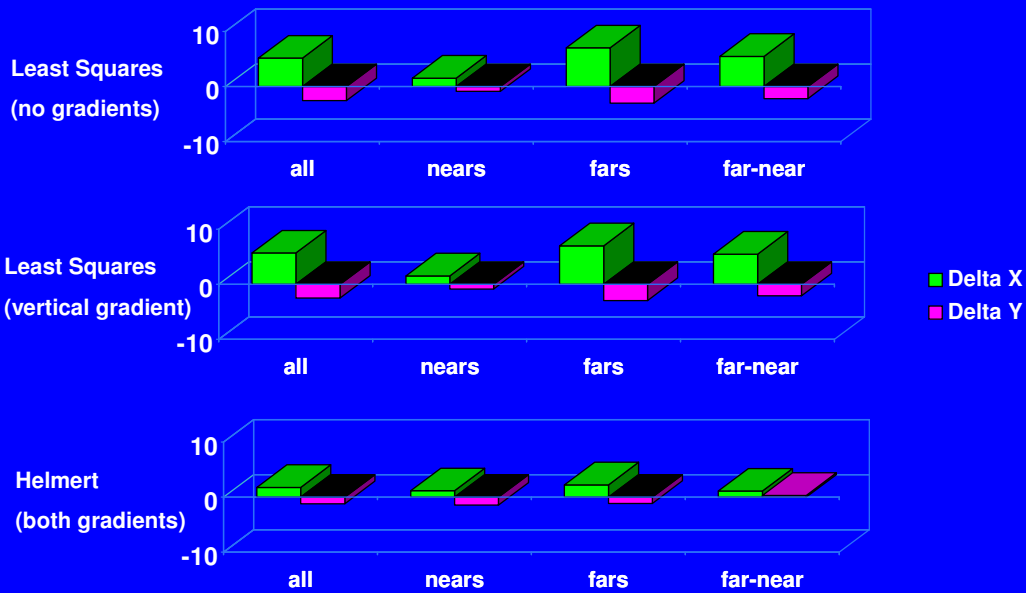
I will show all these comparisons for three algorithms: simple least squares with a linear vertical profile only, simple least squares with a higher-order vertical profile only, and the Helmert algorithm that models both the vertical and lateral gradients.

Simulated-Data Comparisons with Truth



This bar chart and the next are reproduced as numerical tables with more information in the paper for closer examination at your leisure. Comparisons of synthetic data with the truth are first and comparisons of real data with acoustics are next. Split data comparisons on offset are depicted by the fourth pair of bars for each algorithm. On this slide notice that the LS algorithms without the lateral feature have trouble with ΔY shown in maroon. This happens to be where all the lateral gradient is programmed in this synthetic data set. Notice that modeling the vertical gradient in the middle LS algorithm provides only marginal benefit. This is a consequence of the balanced geometry provided by orthogonal shooting. The benefit becomes more pronounced with in-line shooting. Notice that the Helmert algorithm nails the truth over all offset ranges and also in comparison between the nears and the fars.

Real-Data Comparisons with Acoustics



On this slide notice that the LS algorithms have trouble with both ΔX and ΔY coordinates when compared with acoustics, although the near offsets perform much better than the far offsets. On the other hand, the Helmert algorithm compares at the 1 to 2 meter level over all offsets with acoustics. The Helmert nears and fars compare at about one meter or less, better than any comparison with acoustics directly. These results suggest a small in-line bias in the acoustic data. The paper details reasons having to do with delays in the GPS system why this may be so. I encourage you to examine the tables and the accompanying commentary more closely in the paper.

Benefits of Modeling Velocity Gradients

- Better fit to real-world geology
- Decrease predicted error of resulting coordinates
- Better rejection of outliers
- Simultaneous processing of direct and refracted arrivals without human intervention
- Widest possible pick offset range processed
- “Average out” positioning effects of near-surface geological anomalies

In conclusion, I list some of the benefits of modeling velocity gradients. Vertical and lateral velocity gradients are a reality in nature. Explicitly modeling them in the positioning algorithm better fits the geology and decreases coordinate predicted error. Outlier rejection is facilitated. Direct and refracted arrivals are processed together in one adjustment without human intervention. Consequently, the widest possible pick offset range consistent with balanced geometry can be successfully processed. When we are confident that near and far offsets produce statistically-equivalent results we have a strategy for dealing with near-surface geological anomalies. By processing over, through, under and around such anomalies we stand our best chance of "averaging out" their potential effect on our final coordinates.